



MIDDLE EAST TECHNICAL UNIVERSITY

DEPARTMENT OF ELECTRICAL AND ELECTRONICS ENGINEERING

EE 568 Project #3

1 MW Wind Turbine Generator Design and Analysis

GÖKHAN ÇAKAL – 2332120

Introduction

In the project, an axial flux permanent magnet synchronous machine is designed and analysed for the wind turbine generator application. The designed generator has ratings of 1 MW, 20 rpm, 680 V and 850 A. It has double sided rotor structure and it also employs multi-staged design, where several identical designs are stacked in the axial direction in order to decrease the structural mass.

This report is organized as follows. First, the literature survey is presented, where the existing topologies in this field are investigated and several solutions are evaluated for this application. Then, the analytical model of the proposed generator then will be verified by the FEA results, which will be obtained by Ansys Maxwell. At the end, the designed generator will be compared with the existing topologies in the market in the wind energy area.

Part I: Literature Review

Nowadays, researchers are focusing on new machine topologies for renewable energy applications such as wind energy. As the regulations gets tighter, the high efficient and high dynamic machines are getting more attention. In that context, axial flux machines are becoming more popular due to their high torque density.

In the wind turbine generator market and literature, there are several solutions or topologies presented according to different aspects. Direct-drive wind turbine generators have low rotational speed, high torque, and large diameter, which pose remarkable design and manufacturing challenges [1]. Direct-drive synchronous generators can be permanent magnet excited or electrically excited [2]. Permanent magnet excitation has the advantage of improved efficiency and lightweight design at the expense of increased material cost. Radial flux iron-cored generators, which are commonly used in direct-drive wind turbines, are studied in [3]. They suffer from high attraction forces between rotor and stator due to Maxwell stresses, which increase the structural mass of the generator. There are also non-conventional generators such as claw-pole or transverse-flux machines, but they operate at low power factors [4]. Superconducting direct-drive generators are also studied, and they promise high torque densities. However, they are not mature enough for commercialization.

The selected topology in this project, axial flux topology, is heavily studied for wind turbine applications. For example, in [5], 5 kW and 200 rpm permanent magnet axial flux generator is presented and tested for wind energy applications. In [6], 30 kW ironless axial flux generator is optimized. Also, various pole and coil numbers are studies for the design. Additionally, axial flux generator topology is studied in superconducting wind turbine generators. For example, in [7], the authors presented an axial flux homopolar generator topology with 6 MW and 12 rpm ratings. However, the superconducting generators are not mature enough for commercialization.

Part II: Analytical Calculation and Sizing

After quick literature review, we can design analyse the proposed generator. We will start with definition of magnetic loading and electrical loading. Then, the machine constant and torque of the generator will be derived using average tangential stress. Also, other machine parameters such as induced voltage, phase resistance, phase inductance and losses will be derived.

First, let's introduce the topology. The proposed generator is axial flux, double sided, air cored machine with permanent magnet excitation. The stator is sandwiched between two rotor cores. Compared to conventional stranded wired stators, the proposed generator employs flat winding technology, where the stator wires are manufactured from copper sheet by cutting using laser cut or water jet. The simplified presentation of the generator can be seen in the Figure 1.

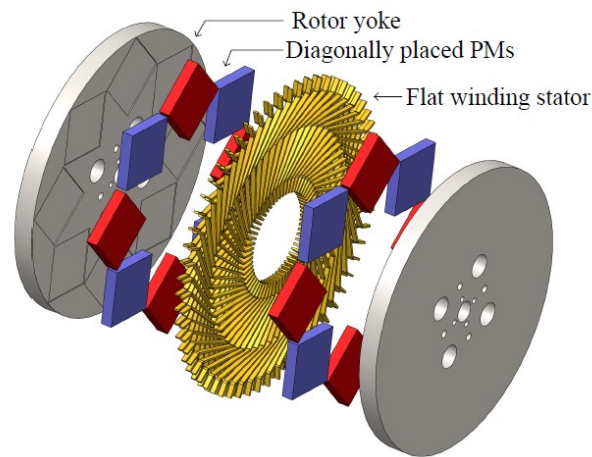


Figure 1: Simplified representation of the proposed generator

The overall specifications of the proposed generator is given in Table 1. The proposed generator employs 46 NdFeB magnets. It's rated speed is 20 rpm. Since there is no gearbox in the system, the rotational speed is low and torque is high.

Table 1: Overall parameters of the generator

Parameter	Value
Rated power	1 MW
Rated speed	20 rpm
Line voltage	680 V
Rated current	840 A
Pole number	46

a) Magnetic loading

First, magnetic loading of the generator will be calculated. To achieve this, the rotor and stator cores are assumed to be infinitely permeable. In the design, N35M grade NdFeB magnets with remanence flux density of 1.212 T are used. Also, in the analysis, it is assumed that there is no leakage and fringing flux in the system, that is, air gap flux density has square shaped magnetic field. The magnetic model of the design is shown in Figure 2 under one pole pair.

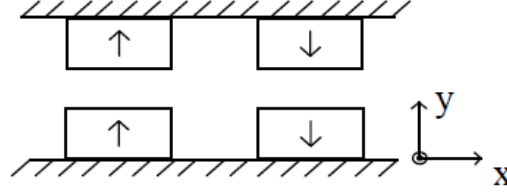


Figure 2: Pole pair representation of the design for magnetic loading calculation

The magnetic equivalent circuit of a magnet can be shown as in Figure 3. It is represented with a voltage source and series added resistance.

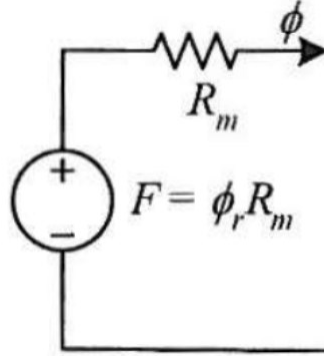


Figure 3: Electrical modelling of a magnet

$$R_m = \frac{l_m}{\mu_0 \mu_r A_m}$$

$$\phi_r = B_r A_m$$

Then, the electrical equivalent of a pole pair can be found easily. Air gap is also modelled as a series added resistance. In this analysis, the cores are assumed to be infinitely permeable, where there is no MMF drop. Then, the electrical circuit model of the machine under one pole can be seen as in Figure 4.

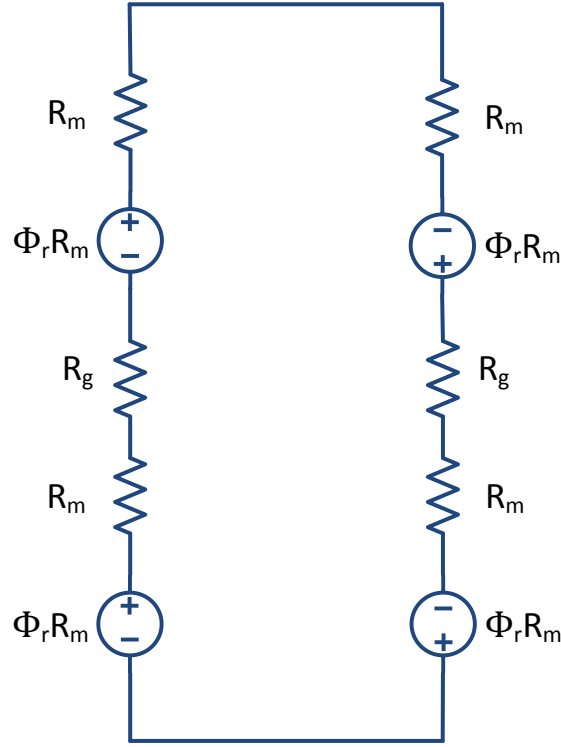


Figure 4: Electrical equivalent of the machine under one pole pair

The analytical calculation of air gap flux density starts with derivation of air gap flux. In the analysis, it is assumed that there is no fringing and leakage flux and air gap flux density has square shape. Then, air gap flux can be derived using electrical equivalent circuit as follows:

$$\phi_m = \phi_g = \frac{4\phi_r R_m}{4R_m + 2R_g} = \frac{2\phi_r R_m}{2R_m + R_g}$$

$$\phi_r = B_r A_m$$

$$R_m = \frac{l_m}{\mu_0 \mu_r A_m}$$

$$R_g = \frac{l_g}{\mu_0 A_g}$$

$$A_m = A_g$$

$$l_m = 36.5 \text{ mm} \text{ and } l_g = 47.3 \text{ mm}$$

$$\phi_g = A_m * 1.212 * \frac{2 * \frac{36.5}{1.05}}{2 * \frac{36.5}{1.05} + 47.3} = 0.712 A_m$$

$$B_g = \frac{\phi_g}{A_g} = \frac{\phi_g}{A_m} = 0.712 \text{ T}$$

It is found that air gap peak flux density is 0.712 T, analytically. Magnetic loading is defined as average of fundamental component of the air gap flux density. It is assumed in our analysis that air gap flux density has square shaped waveform. Its peak of fundamental component can be found as

$$B_{p1} = B_{square} \frac{4}{\pi} \sin\left(\frac{\theta_m}{2}\right)$$

$$B_{p1} = 0.712 \frac{4}{\pi} \sin(90 * 0.8) = 0.873 \text{ T}$$

$$B_{avg} = B_{p1} * \frac{2}{\pi} = 0.873 * \frac{2}{\pi} = 0.556 \text{ T}$$

The magnetic loading of the generator is found to be 0.556 T. The typical magnetic loading for permanent magnet machines is between 0.55-0.8 T. Considering that the design is air cored, the obtained magnetic loading value makes sense.

b) Electrical loading

In the design, novel flat wires are used instead of conventional stranded wires. It has current density of 3.8 A/mm². The cross sectional area of the flat wire is 3x18.6 mm². Therefore, current of a flat wire can be calculated as follows

$$J = 3.8 \text{ A/mm}^2$$

$$A_{wire} = 3 \times 18.6 \text{ mm}^2 = 55.8 \text{ mm}^2$$

$$I_{wire} = J \times A_{wire} = 212 \text{ A}$$

In the design, two stages exist. In each stage, there are two parallel turns. Therefore, for 1 MW machine, the phase current is 848 A and it has line voltage of 680 V. The electrical loading of the generator can be calculated as follows

$$A = \frac{N_{fw} I_{wire}}{2\pi r_{mean}} = \frac{2898 * 212}{2 * \pi * 2.23} = 43.8 \frac{kA}{m}$$

where N_{fw} and r_{mean} are number of flat wires per stage and mean radius, respectively. For PMSM, as a rule of thumb, the electrical loading should be between 35-65 kA/m. Our calculation is coherent with this values.

As a next step, specific machine constant, C_{mech} , can be calculated as follows

$$C_{mech} = \pi^2 * k w_1 * A * B_{avg} = \pi^2 * 0.955 * 43.8k * 0.556 = 230 \frac{kWs}{m^3}$$

c) Average tangential stress and torque

The average tangential stress is calculated as follows

$$\sigma = \frac{AB_{p1} \cos \theta}{\sqrt{2}} = \frac{43.8 * 0.873T * 1}{\sqrt{2}} = 27 \text{ kPa}$$

The torque of the machine can be calculated by tangential stress. However, we should first find the air gap area

$$A_{airgap} = \pi(r_{out}^2 - r_{in}^2) = 4.28 \text{ m}^2$$

where r_{out} and r_{in} are outer and inner radius of the generator, respectively. Then, the torque can be expressed as

$$T_{stage} = \sigma A_{airgap} r_{mean} = 27 \text{ kPa} * 4.28 \text{ m}^2 * 2.23 \text{ m} = 258 \text{ kNm}$$

This value is the torque produced by the single stage of the generator. However, as stated before, the generator is multi-staged and there are two stages. Therefore, total torque can be expressed as

$$T = T_{stage} * n_{stage} = 258 \text{ kNm} * 2 = 515 \text{ kNm}$$

d) Power calculation

The power of the machine is proportional with the speed of the generator. In the design, the rotational speed is set to 20 rpm since we have a direct drive system. Then, the power of the generator can be expressed as

$$P = T * \omega = 515 \text{ kNm} * 20 * \frac{\pi}{30} = 1.08 \text{ MW}$$

e) Back core thickness calculation

As a back core material, Stell1010 can be used. It has saturation flux density around 1.5 T. Then, the back core thickness can be calculated as follows

$$\frac{B_{avg} * A_{pole}}{2} = B_{core} * A_{core}$$

$$h_{core} = \frac{B_{avg} A_{airgap}}{2 \text{ pole } B_{coremax} (r_{out} - r_{in})} = \frac{0.556T * 4.28 m^2}{2 * 46 * 1.5T * (2.385m - 2.0796m)} = 56 \text{ mm}$$

f) Electrical parameters

Other electrical parameters of the generator can be calculated easily with the derived expressions. Let's first derive the line voltage and phase voltage. In order to achieve this, we should first derive the line current of the generator. It is found that a flat wire carries 212 A. There are two parallel turns per stage and 2 stages. Therefore, the line or phase current can be calculated as

$$I_{wire} = 212 \text{ A}$$

$$I_{ph} = I_{wire} * 4 = 848 \text{ A}$$

Then, using previously derived power equation, line and phase voltages can be calculated as

$$V_{line} = \frac{P}{\sqrt{3} I_{ph}} = \frac{1.08 \text{ MW}}{\sqrt{3} * 848A} = 735 \text{ V}_{rms}$$

$$V_{ph} = \frac{V_{line}}{\sqrt{3}} = 424 \text{ V}_{rms}$$

These are close to our specifications, which is 400 V phase and 690 V line voltages. Now, we can derive the phase resistance and copper losses of the design. In order to achieve this, let's first focus on the flat wire dimensions as given in Figure 5.

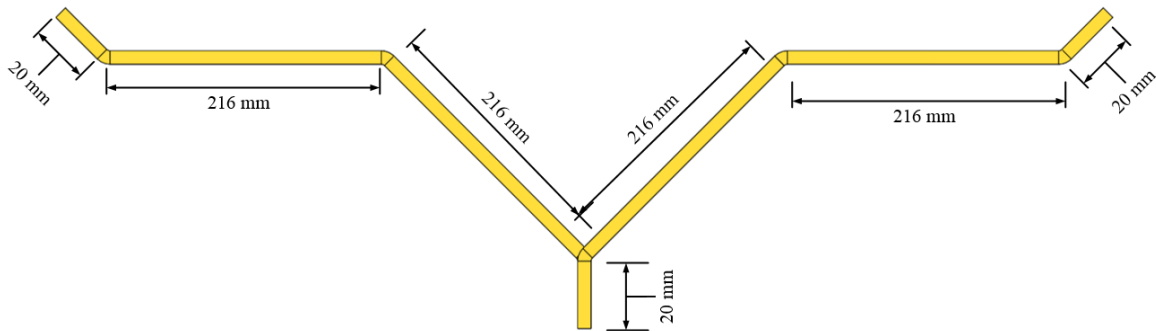


Figure 5: Flat wire dimensions

Then, a single flat wire has the total length of

$$l_{fw} = 0.944 \text{ m}$$

There are 21 loops connected in series in a phase, which is composed of 23 flat wires each. Therefore, in a phase, there are 483 flat wires connected in series. The total length can be calculated as

$$l_{ph-series} = l_{fw} * 483 = 456 \text{ m}$$

The resistivity of copper and flat wire cross sectional area are as follows.

$$\rho_{cu} = 2.026 \times 10^{-8} \Omega m$$

$$A_{wire} = 55.8 \text{ mm}^2$$

Then, the resistivity of series connected loops can be calculated as

$$R_{series} = \frac{\rho l_{ph-series}}{A_{wire}} = \frac{2.026 \times 10^{-8} \Omega m * 456 \text{ m}}{55.8 \text{ mm}^2} = 168 \text{ m}\Omega$$

Remember that there are two parallel connected stages and two parallel turns per stage. Therefore, overall phase resistance can be calculated as

$$R_{ph} = \frac{R_{series}}{4} = 41 \text{ m}\Omega$$

Then, the copper loss of the generator is calculated as

$$P_{cu} = 3 * I_{ph}^2 * R_{ph} = 3 * 848^2 * 41 \text{ m} = 89 \text{ kW}$$

As a next step, magnetizing inductance of the generator can be calculated. Referencing to the lecture notes, the total magnetizing inductance of the generator is as follows

$$L_m = \frac{6 \mu_0 r_{out}(r_{out} - r_{in})(k_w * N_s)^2}{\pi p^2 g_{cl}} = \frac{6 \mu_0 2.385 (2.385 - 2.0796)(0.955 * 21)^2}{\pi 23^2 0.0048}$$

$$L_m = 280 \mu H$$

g) Mechanical parameters

As a next step, mechanical parameters of the generator can be defined. First, let's define the air gap clearance. The air gap clearance of the generator is set to 0.1% of the rotor diameter as follows

$$g_{cl} = 2 * r_{out} * \frac{0.1}{100} = 4.8 \text{ mm}$$

The axial length of the generator can be obtained as a next step. To achieve this, remember that there are two stages in the design stacked in the axial direction. Also, note that the back core between two stages can be thin because the flux will go through in axial direction in this rotor core. Therefore, the total axial length of the generator is calculated as

$$l_{axial} = 370 \text{ mm}$$

Then, the aspect ratio of the generator, defined as the ratio of axial length to the machine diameter, can be defined as follows

$$x = \frac{l_{axial}}{2r_{out}} = \frac{0.37}{4.77} = 0.08$$

Note that this value is quite small compared to radial flux machines. This is expected since the axial flux machines have small axial length and large diameter. Especially considering that the machine is direct-driven, the diameter is large and the aspect ratio is small.

Part III: FEA Modelling

At the last part of the report, finite element analysis results will be presented. The obtained results will be compared with analytical solutions and comments will be made. In the analysis, Ansys Maxwell 3D solver is used. The model shown in Figure 6 is used in the simulation. In order to decrease the computational load, pole symmetry of the model is preferred. Also, it is stated that the design is two staged. Only one stage of the design is simulated and symmetry boundary condition is applied. Lastly, it is very challenging and time consuming to mesh all the flat wires in the design. Remember that there are 2898 flat wires per stage. Again, to decrease the computational load, only a few flat wires are presented in the analysis and simulation is adapted accordingly to give the values for the actual model.

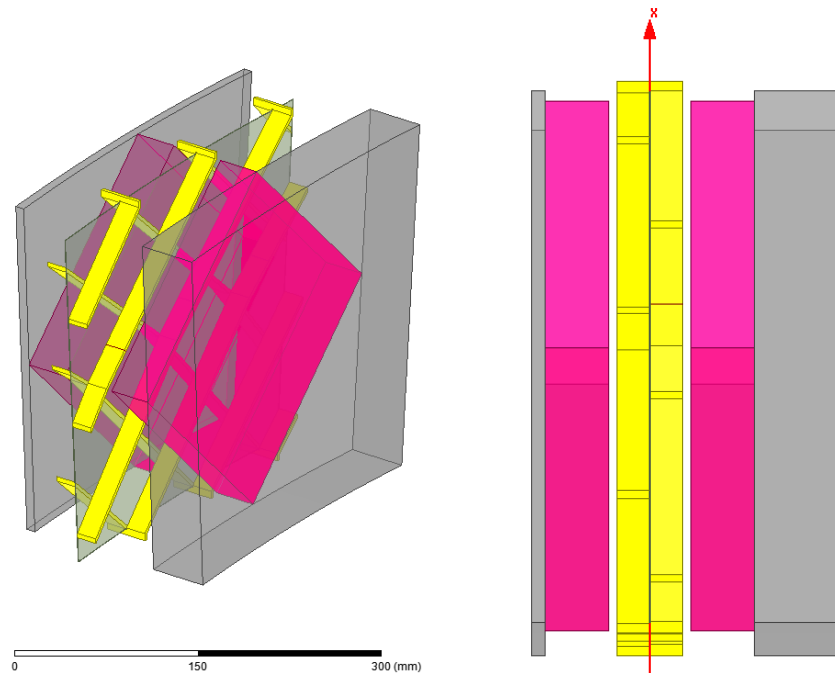


Figure 6: Simulated model for FEA

a) Magnetic field results

In order to evaluate the analytical results, finite element solution is obtained for the proposed generator. Firstly, the accuracy of the magnetic field model and magnetic loading is questioned. In order to achieve this, using ANSYS Maxwell, the model shown in Figure 2 is solved. The results are shown in Figure 7.

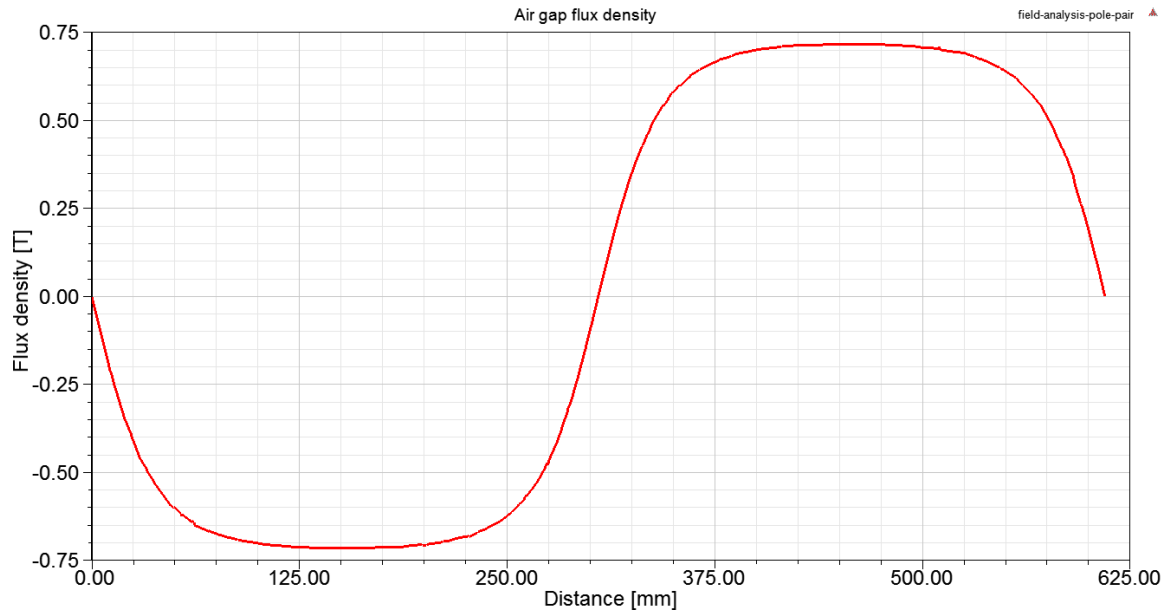


Figure 7: Air gap flux density over one pole-pair

When the FFT analysis is conducted on the air gap flux density distribution in Figure 7, it is observed the average value of the fundamental component, that is magnetic loading, is 0.539 T. Analytically, we found that magnetic loading is 0.556 T. Therefore, there is around 3% difference, which is mainly caused by the assumption that there is no leakage and fringing effect and there is no saturation in the cores. In overall, the obtained results are in good agreement with analytical calculations.

b) Flux density distribution

The design is air cored, thus, there is no iron at the stator. The saturation phenomenon occurs only on rotor cores. In Figure 8, flux density distribution on the rotor cores are shared. The selected core material starts to saturate around 1.5 T. In the analysis, it is shown that the core material is not saturated under rated operation, validating the core thickness calculation. Additionally, note that the rotor core on the left is the core between two stages. Since the flux goes in the axial direction in this part, there is no saturation observed, as expected. Additionally, in Figure 9, flux vectors are shown.

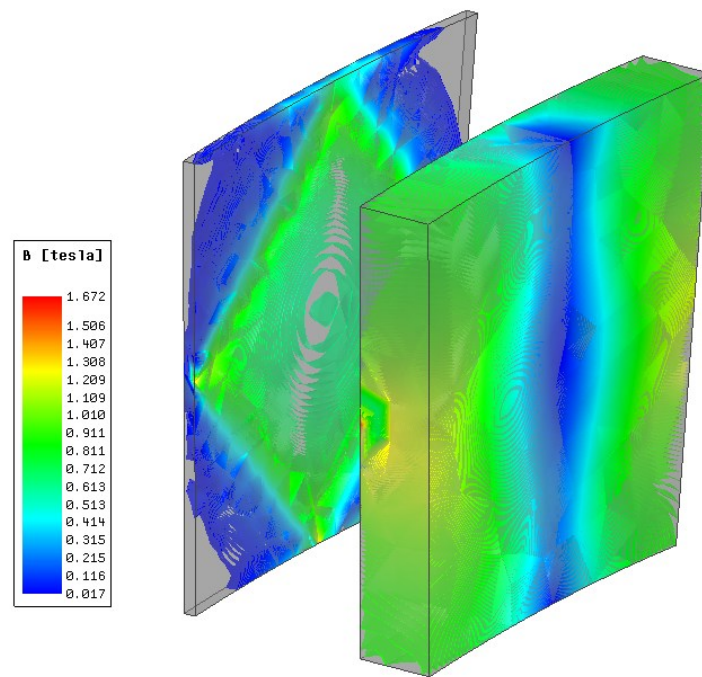


Figure 8: Flux density distribution on the rotor cores

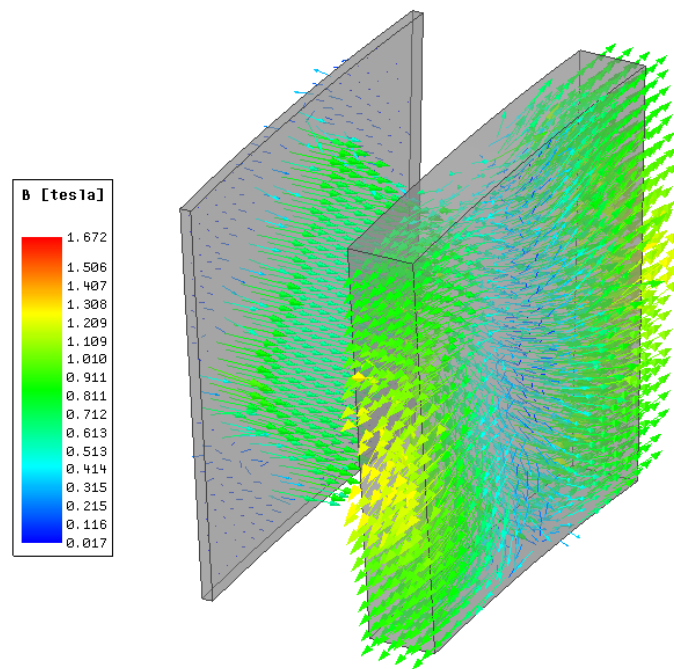


Figure 9: Flux vectors on the cores

c) Phase resistance

The phase resistance can be obtained from the copper losses. In order to achieve this, we will first simulate the machine at rated operation, and measure the solid losses on the coils. These losses include both AC losses such as eddy current losses and conduction losses. There is no direct separation between these two losses. In order to separate them, we first obtain solid losses during rated operation, which is seen in Figure 10. It has average of 107 kW and includes AC and conduction losses. When we operate the machine again at no load condition, ie. zero current, we can obtain solid losses as in Figure 11. It has average value of 24 kW and includes only AC losses. Then, the conduction losses at rated operation can be calculated as

$$P_{cu} = 107 \text{ kW} - 24 \text{ kW} = 83 \text{ kW}$$

This value is close to the analytical conduction loss calculation of 89 kW, with 7% difference. This is mainly resulted from the temperature effect, which is included in the analytical calculation but not included in the FEA. Then, phase resistance by FEA can be derived as

$$R_{ph-FEA} = 38 \text{ m}\Omega$$

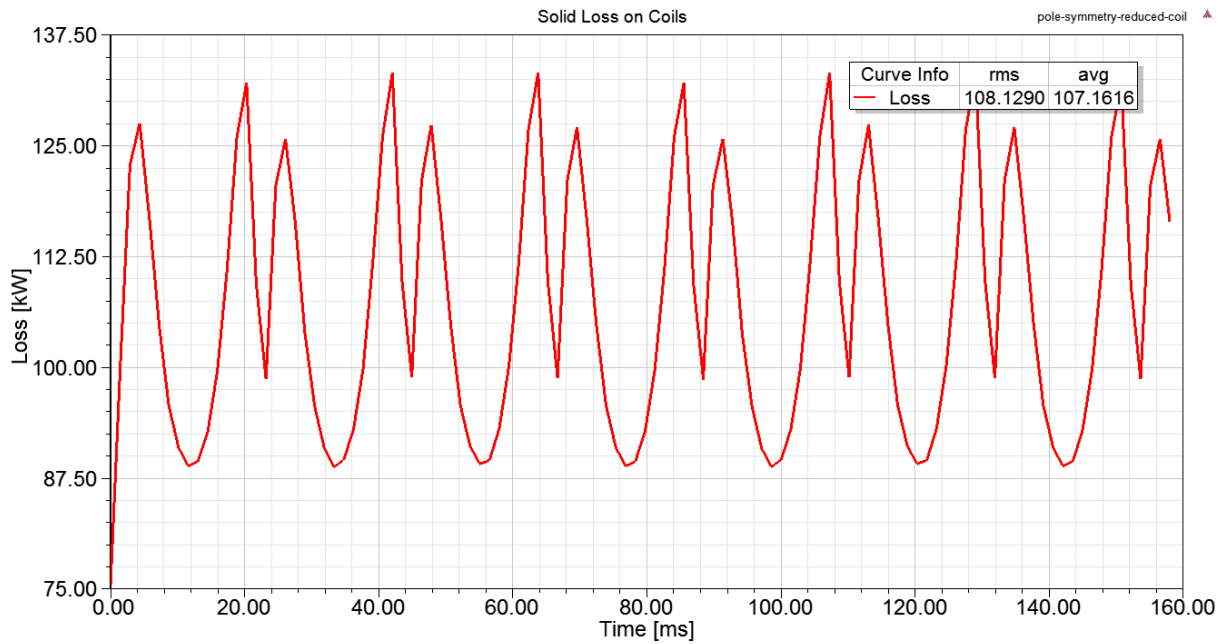


Figure 10: Solid losses including conduction and AC losses

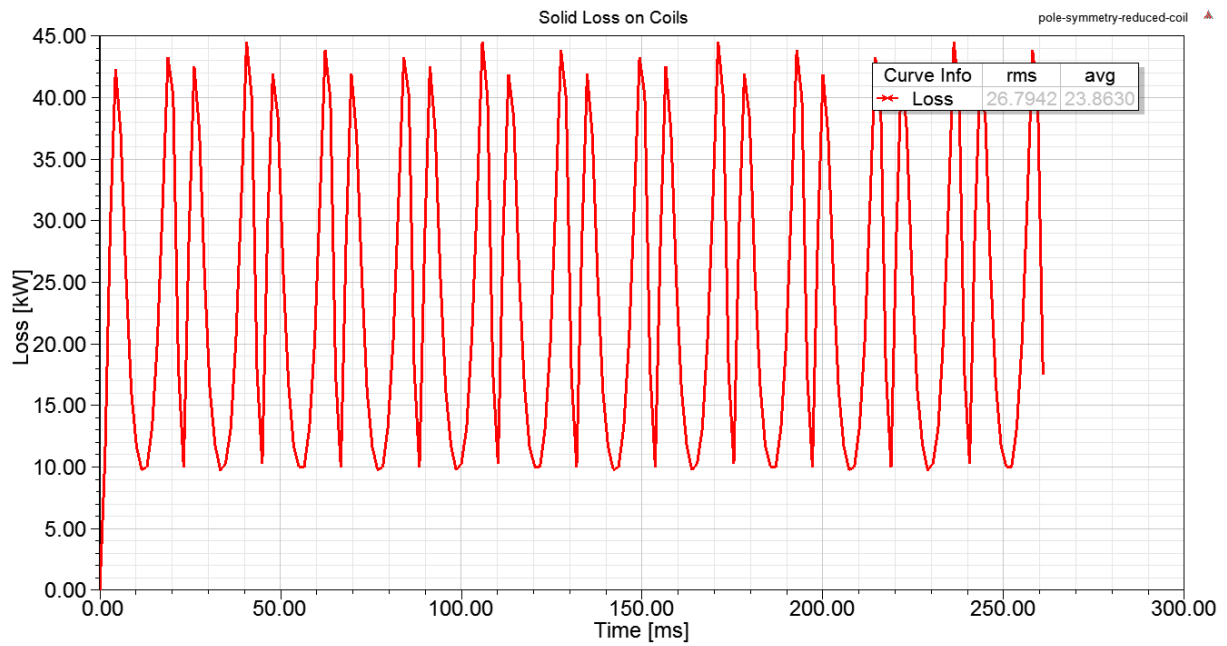


Figure 11: Solid losses at no load (zero current)

d) Phase voltages

Analytically, we obtained that the phase voltage is 424 V_{rms}. Using FEA tool, the induced phase voltage is obtained as in Figure 12. It is seen that the results have rms value of 412 V. The analytical and FEA results have less than 3% difference, which is acceptable. The small difference is mainly caused by the approximations in the analytical model.

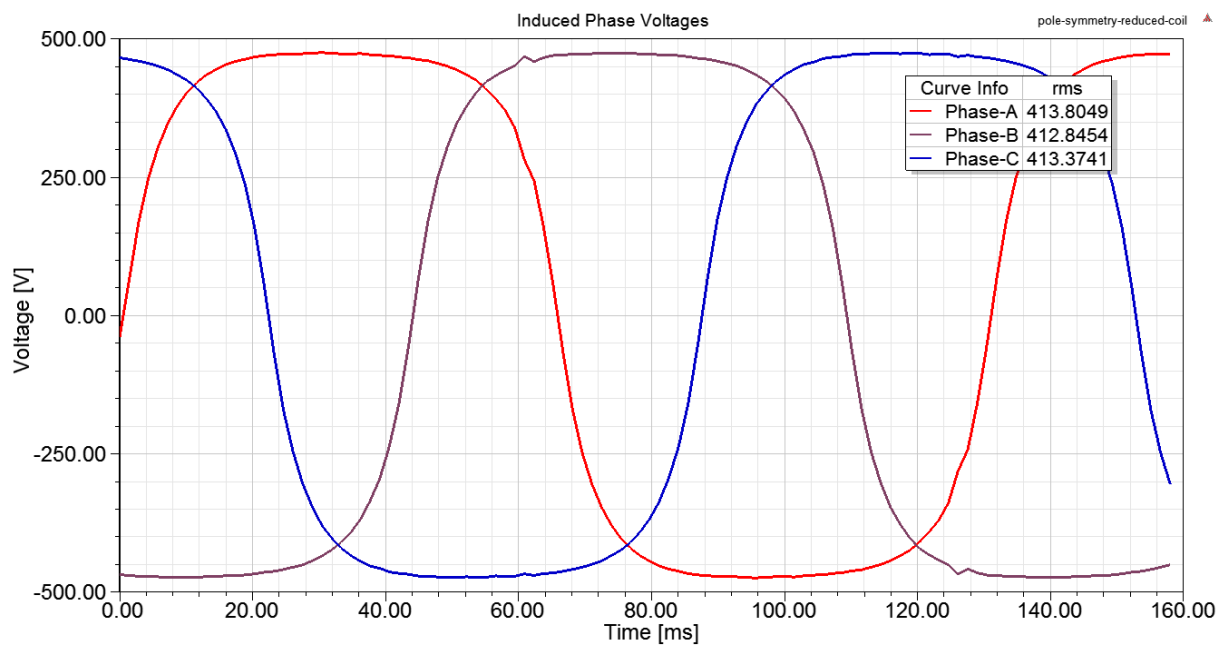


Figure 12: Induced phase voltages by FEA

e) Torque

Analytically, the torque of the machine is calculated as 515 kNm. Using FEA tools, as in Figure 13, it has rated value of 473 kNm. The difference is around 8%. This shows that the analytical model has room to improve for the accurate results.

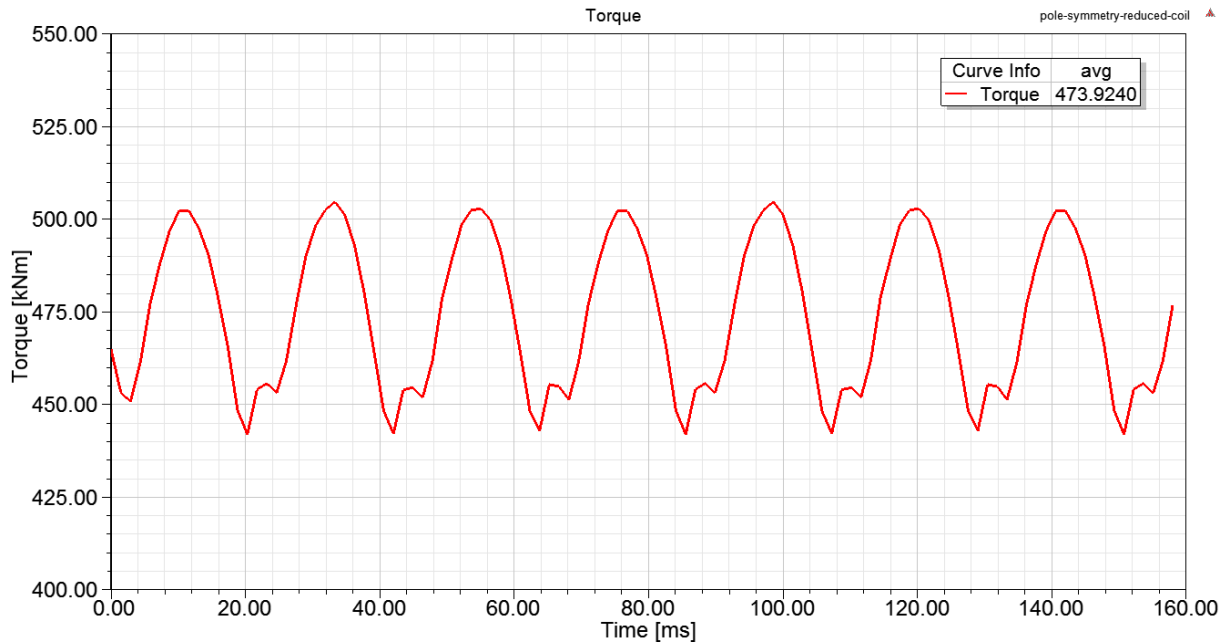


Figure 13: Torque by FEA

f) Efficiency calculation at full and half load

The efficiency of the generator will be calculated using output power and losses obtained by FEA. To achieve this, at half current, the machine is simulated. The results are tabulated in Table 2. In the table, total loss includes both conduction and AC losses of the design. It is observed that at half load, the generator works more efficient with slight difference.

Table 2: Efficiency calculation at half and full loads by FEA

	Torque	Speed	Power	Total loss	Efficiency
Half load	231 kNm	20 rpm	484 kW	43 kW	91.8%
Full load	993 kNm	20 rpm	993 kW	107 kW	90.3%

Part IV: Comparison and Discussion

The general comments and comparisons between analytical and FEA results are given mainly in previous part. However, similar findings can be pointed out here also. In general, the results of the analytical model are in good agreement with FEA results. The most obvious difference shows itself in the resistance and conduction loss calculation, which was around 8%. This difference is mainly caused by the temperature effect. In FEA, the temperature effect is not included, that is the operating temperature is set to 25 deg. However, in the analytical model, this effect is also included and thus this difference is observed.

It was interesting to discover how design parameters are defined in the axial flux machines, such as electrical loading, magnetic loading or machine constant. In the lecture, we saw them for the conventional radial flux machines. With simple modifications, we derived these expressions for the axial flux machines. Also, for the novel flat winding topology, it was interesting to discover how electrical loading is defined, although there are still unclear points to be discussed. In overall, these design parameters are within the conventional ranges defined for the radial flux machines.

Overall design parameters of the proposed 1 MW generator for the wind energy applications are shared in Table 3.

Table 3: Overall design parameters of the machine

Parameter	Value
Rated power	1 MW
Rotational speed	20 rpm
Diameter	4.8 m
Voltage	680 V
Current	850 A
Number of poles	46
Torque	480 kNm
Axial length	0.36 m
Aspect ratio	0.075
Efficiency	90%
Copper losses	75 kW
Eddy losses	31 kW
Active mass	10.4 t
Structural mass	5.6 t
Total mass	16.0 t
Torque density	29.8 Nm/kg
Electrical frequency	7.7 Hz
Number of stages	2
Number of parallel turns per stage	2
Current density	3.8 A/mm ²
Flat wire width	18.6 mm
Flat wire thickness	3 mm
Total cost	€203k
Air gap peak flux density	0.85 T

Table 4: Comparison of the optimum design with existing generators

Study	Generator type	Power, MW	Speed, rpm	Torque, kNm	Number of stages	Active mass, t	Structural mass, t	Total mass, t	Torque density by active mass, Nm/kg	Torque density by total mass, Nm/kg
Li <i>et al.</i>	Radial flux PM	0.75	29	250	1	3.1	-	-	79.7	-
This study	Axial flux PM	1	20	477	2	10.4	5.6	16.0	46.0	29.8
McDonald <i>et al.</i>	Axial flux PM	1	12	798	4	18.6	6.9	25.5	42.9	31.3
Maples <i>et al.</i>	Radial flux PM	1	26	367	1	-	-	17.4	-	21.0
Versteegh	Radial flux PM	1.5	18	796	1	16.7	20.8	37.5	47.7	21.2
Bang	Radial flux PM	2	20	979	1	14.6	10.4	25.0	67.0	39.2

In Table 4, the optimum design is compared with wind power generators presented in the literature. In comparison study, direct drive permanent magnet generators with power ratings between 0.75 MW and 2 MW are considered. Torque density (Nm/kg) is selected as the performance parameter. Some of the publications do not include active, structural, or total mass data. Therefore, two definitions of torque density considering either active or total mass are made. The results show that the optimum design presented in this paper has comparable torque density compared to other studies. Also, it is seen that the presented structural model and multi-staged design creates a significant advantage in torque density by total mass in the comparative study.

References

- [1] A. L. F. P. S. B. A. B. M. D. M. M. Tassarolo, «Design for manufacturability of an off-shore direct-drive wind generator: An insight into additional loss prediction and mitigation,» *IEEE Transactions on Industry Applications*, cilt 3, no. 52, pp. 4831-4842, 2017.
- [2] E. S. R. N. T. I. A. S. M. Taherian-Fard, «Wind turbine drivetrain technologies,» *IEEE Transactions on Industry Applications*, cilt 2, no. 56, pp. 1729-1743, 2020.
- [3] T. K. J. C. R. W. F. G. L. de Paula Machado Bazzo, «Multiphysics design optimization of a permanent magnet synchronous generator,» *IEEE Transactions on Industrial Electronics*, cilt 12, no. 64, pp. 9815-9823, 2017.
- [4] H. F. J. J. B. A. A. A. K. Polinder, «Trends in wind turbine generator systems,» *IEEE Journal of Emerging and Selected Topics in Power Electronics*, cilt 1, no. 3, pp. 174-185, 2013.
- [5] B. Chalmers ve E. Spooner, «An axial-flux permanent-magnet generator for a gearless wind energy system,» *IEEE Transactions on Energy Conversion*, cilt 2, no. 14, pp. 14-19, 1999.
- [6] A. Daghigh, H. Javadi ve H. Torkaman, «Design Optimization of Direct-Coupled Ironless Axial Flux Permanent Magnet Synchronous Wind Generator With Low Cost and High Annual Energy Yield,» *IEEE Transactions on Magnetics*, cilt 9, no. 1, p. 52, 2016.
- [7] O. Keysan ve M. A. Mueller, «A Homopolar HTSG Topology for Large Direct-Drive Wind Turbines,» *IEEE Transactions on Applied Superconductivity*, cilt 12, no. 5, pp. 3523-3531, 2011.